Mon. Not. R. Astron. Soc. **000**, 000–000 () Printed 1 February 2008 (MN LATEX style file v2.2)

The status of Galactic field λ Boötis stars in the post-Hipparcos era

E. Paunzen[1,2], I.Kh. Iliev[3], I. Kamp[4], I.S. Barzova[3]
1-Institut für Astronomie der Universität Wien, Türkenschanzstr. 17, 1180 Wien, Austria
2-Zentraler Informatikdienst der Universität Wien, Universitätsstr. 7, 1010 Wien, Austria
3-Institute of Astronomy, National Astronomical Observatory, P.O. Box 136, 4700 Smolyan, Bulgaria
4-Leiden Observatory, Niels Bohrweg 2, PO Box 9513, 2330 RA Leiden, The Netherlands

arXiv:astro-ph/0207488v1 23 Jul 2002

1 February 2008

ABSTRACT
The λ Boötis stars are Population I, late B to early F-type stars, with moderate to extreme (up to a factor 100) surface underabundances of most Fe-peak elements and solar abundances of lighter elements (C, N, O, and S). To put constraints on the various existing theories that try to explain these peculiar stars, we investigate the observational properties of λ Boötis stars compared to a reference sample of normal stars. Using various photometric systems and Hipparcos data, we analyze the validity of standard photometric calibrations, elemental abundances, and Galactic space motions.

There crystallizes a clear picture of a homogeneous group of Population I objects found at all stages of their main-sequence evolution, with a peak at about 1 Gyr. No correlation of astrophysical parameters such as the projected rotational velocities or elemental abundances with age is found, suggesting that the a-priori unknown mechanism, which creates λ Boötis stars, works continuously for late B to early F-type stars in all stages of main-sequence evolution. Surprisingly, the sodium abundances seem to indicate an interaction between the stars and their local environment.

Key words: Stars: λ Bootis – Stars: chemically peculiar – Stars: early-type

1 INTRODUCTION

Knowledge of the evolutionary status of the members of the λ Boötis group is essential to put tight constraints on the astrophysical processes behind this phenomenon. We have chosen the following working definition as group characteristics: late B- to early F-type, Population I stars with apparently solar abundances of the light elements (C, N, O and S) and moderate to strong underabundances of Fe-peak elements (see Faraggiana & Gerbaldi 1998 for a critical summary of the various definitions). Only a maximum of about 2% of all objects in the relevant spectral domain are believed to be λ Boötis-type stars (Paunzen 2001). That already suggests either that the mechanism responsible for the phenomenon works on a very short time-scale (10^6 yrs) or else the general conditions for the development are very strict.

We know already of a few λ Boötis stars in the Orion OB1 association and one candidate in NGC 2264 (Paunzen 2001), for both of which $\log t \approx 7.0$. The evolutionary status for two λ Boötis-type spectroscopic-binary systems (HD 84948 and HD 171948) has been determined as very close to the Zero Age Main Sequence (ZAMS hereafter) for HD 171948 and to the Terminal Age Main Sequence (TAMS hereafter) for HD 84948 (Iliev et al. 2002). The results for the other Galactic field stars are not clear.

In 1995, Iliev & Barzova summarized the evolutionary status of 20 λ Boötis stars (and Vega) using Strömgren $uvby\beta$ photometric data. They concluded that most of the stars studied are in the middle of their main-sequence evolution, with only a few objects near the ZAMS.

Paunzen (1997) investigated the parallaxes measured by the Hipparcos satellite for a sample of λ Boötis-type stars in order to derive luminosities, masses and ages for 18 objects in common with Iliev & Barzova (1995). He found no systematic influence of the distance, effective temperature, metallicity and rotational velocity on the difference between photometrically calibrated absolute magnitudes and those derived from Hipparcos parallaxes. Six objects were found to be very close to the ZAMS and a hypothesis was proposed that all other stars are in their Pre-Main-Sequence (PMS hereafter) phase.

Later on, Bohlender, Gonzalez & Matthews (1999) and Faraggiana & Bonifacio (1999) challenged that hypothesis with plausible arguments such as the unusually vigorous star-forming activity that it implied in the solar neighbourhood and a statistical analysis of normal-type stars.

Already Gray & Corbally (1998) stated that the λ Boötis phenomenon can be found from very early stages to well into the main-sequence life of A-type stars. That conclusion was based on the incidence of λ Boötis stars among very young A-type stars, which is not very different from the incidence among Galactic field stars.

In this paper we present a much more extensive investigation, including the data of the Hipparcos satellite. With the help of photometric data of the Johnson *UBV*, Strömgren *uvbyβ* and Geneva 7-colour systems, different calibrations of the absolute magnitude, effective temperature and surface gravity are applied and compared.

From evolutionary models (Claret 1995), masses and ages are estimated. They are compared with those derived by Iliev & Barzova (1995) and Paunzen (1997).

As a further step, the proper motions of λ Boötis stars are used to calculate space velocities. That very important information should help further to sharpen the group properties and to sort out probably misclassified stars.

Another point investigated is the question as to whether there exists a typical abundance pattern for the λ Boötis group. Heiter (2002) and Heiter et al. (2002) tried to shed more light on the abundance pattern in the context of the proposed theories. We have searched for correlations of the individual abundances with, especially, mass and age.

However, we will not comment on our results in the context of the developed theories and models, because they still depend on too many free parameters. The aim of this paper is not to promote one of the suggested theories but rather to find strict observational constraints which should be incorporated into future theoretical investigations.

2 PROGRAM STARS AND THEIR ASTROPHYSICAL PARAMETERS

The program stars were taken from the lists of Gray & Corbally (1998) and Paunzen (2001), with the omission of apparent spectroscopic binary systems (e.g. HD 38545, HD 64491, HD 111786, HD 141851 and HD 148638) as well as of HD 191850 for which no β measurement is available so no reliable astrophysical parameters could be derived from the Strömgren photometric system. A further critical assessment of the literature was performed in order to reject probable non-members and ill-defined objects. In total, 57 well established λ Boötis stars were chosen.

The photometric data were taken from the General Catalogue of Photometric Data (GCPD; http://obswww.unige.ch/gcpd/) as well as from the Hipparcos and Tycho database. If available, averaged and weighted mean values were used.

The following calibrations for the individual photometric systems were used to derive the effective temperatures and surface gravities:

- Johnson *UBV*: Napiwotzki, Schönberner & Wenske (1993)
- Strömgren *uvbyβ*: Moon & Dworetsky (1985) and Napiwotzki et al. (1993)
- Geneva 7-colour: Kobi & North (1990) and Künzli et al. (1997)

The reddening and absolute magnitudes were estimated by use of the Strömgren *uvbyβ* system. The calibrations for the Johnson *UBV* and Geneva 7-colour system need an a-priori knowledge of the reddening which is not easy to estimate.

An independent way to derive the interstellar reddening maps is to use data from open clusters as well as Galactic field stars. Several different models have been published in the literature (Arenou, Grenon & Gómez 1992, Hakkila et al. 1997). Chen et al. (1998) compared the results from Arenou et al. (1992) and those derived from Hipparcos measurements, and found an overestimation in previously published results for distances less than 500 pc. They consequently proposed a new model for Galactic latitudes of $\pm 10^{\circ}$, but otherwise find excellent agreement with the model by Sandage (1972). We use here the model proposed by Chen et al. (1998) who corrected previous models by Arenou et al. (1992) on the basis of the Hipparcos data. The values from the calibration of the Strömgren *uvbyβ* and the model by Chen et al. (1998) are in very good agreement. To minimize possible inconsistencies we have averaged the values from both approaches.

The Hipparcos parallaxes were converted directly into absolute magnitudes. The latter were averaged (using weights based on the standard errors) with the absolute magnitudes derived from the photometric calibrations. With the absolute bolometric magnitude of the Sun $(M_{\rm Bol})_{\odot} = 4.75$ mag (Cayrel de Strobel 1996) and the bolometric correction taken from Drilling & Landolt (2000), luminosities ($\log {\rm L}_*/{\rm L}_{\odot}$) were calculated (Table 1).

We have also corrected our data for the so-called 'Lutz–Kelker effect' (Koen 1992), an overestimation of parallaxes owing to random errors. Oudmaijer, Groenewegen & Schrijver (1998) showed that that bias has to be taken into account if individual absolute magnitudes from Hipparcos parallaxes are calculated.

The projected rotational velocities were taken from Uesugi & Fukuda (1982), Stürenburg (1993), Abt & Morrell (1995), Holweger & Rentzsch-Holm (1995), Chernyshova et al. (1998), Heiter et al. (1998), Paunzen et al. (1999a,b), Kamp et al. (2001), Solano et al. (2001), Andrievsky et al. (2002) and Heiter (2002). If possible the individual values were averaged with weights in accordance with the listed standard errors.

As the next step, we have used the post-MS evolutionary tracks and isochrones from Claret (1995) to estimate the individual masses and ages for our program stars. The models were calculated with solar abundances. That is justified because the abundance pattern found for the λ Boötis stars must be restricted to the surface only: almost all of them would lie below the Population II ZAMS which would be applicable if they were metal-poor throughout. Table 2 lists the masses together with minimum and maximum ages, which are not necessarily equally spaced owing to the shape of the isochrones. Since the lifetime for a star on the MS is dependent on its mass, we have transformed the ages thus determined into relative ones ($t_{\rm rel}$) in the following way. For our sample we find masses (Table 2) from 1.6 to 2.5 ${\rm M}_{\odot}$, which correspond to times on the MS of 2.2 Gyr down to 700 Myr. The relative age is zero for an object which just arrived at the ZAMS and unity for stars at the TAMS. We have taken into account the error of the estimated mass as well as the error box of the calibrated ages.

Table 1. Photometric data, stellar parameters and calibrated values for the program stars. In parenthesis are the errors in the final digits of the corresponding quantity.

HD	HR	HIP	V [mag]	$B-V$ [mag]	$b-y$ [mag]	$A_{\rm V}$ [mag]	$v \sin i$ [kms^{-1}]	$T_{\rm eff}$ [K]	$\log g$(phot) [dex]	$M_{\rm V}$ [mag]	$\log {\rm L}_*/{\rm L}_\odot$
319	12	636	5.934	0.141	0.079	0.004	60	8020(135)	3.74(8)	1.27(19)	1.45(8)
6870		5321	7.494	0.246	0.164	0.000	165	7330(102)	3.84(11)	2.29(42)	1.02(17)
7908		6108	7.288	0.272	0.192	0.000		7145(87)	4.10(12)	2.60(18)	0.90(7)
11413	541	8593	5.940	0.147	0.105	0.004	125	7925(124)	3.91(21)	1.49(10)	1.35(4)
13755		10304	7.844	0.318	0.181	0.000		7080(161)	3.26(10)	0.93(10)	1.57(4)
15165		11390	6.705	0.333	0.191	0.010	90	7010(167)	3.23(10)	1.12(16)	1.50(6)
23392		17462	8.260	0.020	0.014	0.094		9805(281)	4.35(9)	1.43(30)	1.45(12)
24472		18153	7.092	0.304	0.214	0.003		6945(131)	3.81(16)	2.14(11)	1.09(5)
30422	1525	22192	6.186	0.190	0.101	0.014	135	7865(108)	4.00(20)	2.35(1)	1.01(1)
31295	1570	22845	4.648	0.085	0.044	0.063	115	8920(177)	4.20(1)	1.66(22)	1.32(9)
35242	1777	25205	6.348	0.122	0.068	0.042	90	8250(103)	3.90(14)	1.75(22)	1.26(9)
54272			8.800	0.261	0.214	0.000		7010(217)	3.83(10)	2.33(30)	1.01(12)
74873	3481	43121	5.890	0.115	0.064	0.078	130	8700(245)	4.21(11)	1.82(1)	1.24(1)
75654	3517	43354	6.384	0.242	0.161	0.012	45	7350(104)	3.77(11)	1.83(12)	1.20(5)
81290		46011	8.866	0.332	0.254	0.124	55	6895(214)	3.82(28)	1.85(30)	1.20(12)
83041		47018	8.927	0.294	0.223	0.161	95	7120(208)	3.76(20)	1.70(30)	1.26(12)
83277		47155	8.304	0.311	0.226	0.131		7000(189)	3.67(18)	1.49(29)	1.35(12)
84123		47752	6.840	0.297	0.235	0.040	20	7025(175)	3.73(17)	1.58(15)	1.31(6)
87271		49328	7.120	0.172	0.151	0.008		7515(232)	3.43(10)	1.02(8)	1.53(3)
90821			9.470	0.105	0.068	0.013	150	8190(79)	3.73(10)	0.74(30)	1.66(12)
91130	4124	51556	5.902	0.109	0.073	0.000	135	8135(98)	3.78(10)	1.36(26)	1.42(11)
101108		56768	8.880	0.179	0.114	0.006	90	7810(80)	3.90(18)	1.33(30)	1.42(12)
102541		57567	7.939	0.230	0.163	0.097		7665(168)	4.22(16)	2.34(21)	1.01(9)
105058		58992	8.900	0.183	0.129	0.009	140	7740(171)	3.77(30)	0.86(30)	1.60(12)
105759		59346	6.550	0.218	0.142	0.000	120	7485(102)	3.65(10)	1.35(21)	1.40(8)
106223		59594	7.431	0.288	0.228	0.015	90	6855(247)	3.49(18)	1.83(45)	1.22(18)
107233		60134	7.353	0.255	0.192	0.048	95	7265(143)	4.03(10)	2.64(13)	0.88(5)
109738			8.277	0.198	0.161	0.073		7610(145)	3.90(13)	1.85(30)	1.20(12)
110377	4824	61937	6.228	0.195	0.120	0.000	170	7720(89)	3.97(14)	1.96(11)	1.16(5)
110411	4828	61960	4.881	0.077	0.040	0.045	165	8930(206)	4.14(14)	1.90(28)	1.22(11)
111005		62318	7.959	0.376	0.224	0.009		6860(66)	3.72(10)	1.76(53)	1.24(21)
111604	4875	62641	5.886	0.160	0.112	0.000	180	7760(149)	3.61(25)	0.48(7)	1.75(3)
120500		67481	6.600	0.131	0.068	0.017	125	8220(70)	3.86(10)	0.85(34)	1.62(13)
120896		67705	8.495	0.296	0.166	0.000		7260(89)	3.76(10)	1.90(30)	1.18(12)
125162	5351	69732	4.186	0.084	0.051	0.039	115	8720(156)	4.07(9)	1.71(23)	1.28(9)
125889			9.849	0.241	0.206	0.108		7275(175)	3.88(9)	2.32(30)	1.01(12)
130767		72505	6.905	0.042	0.002	0.000		9195(220)	4.10(8)	1.27(1)	1.48(1)
142703	5930	78078	6.120	0.240	0.182	0.021	100	7265(150)	3.93(12)	2.41(12)	0.97(5)
142944			7.179	0.293	0.201	0.013	180	7000(125)	3.19(4)	0.80(30)	1.62(12)
149130		81329	8.498	0.342	0.233	0.109		6945(103)	3.49(5)	1.51(30)	1.34(12)
153747		83410	7.420	0.140	0.098	0.128		8205(90)	3.70(24)	1.24(30)	1.46(12)
154153	6338	83650	6.185	0.284	0.199	0.020		7055(120)	3.56(6)	1.86(29)	1.19(11)
156954		84895	7.679	0.294	0.200	0.050	50	7130(93)	4.04(13)	2.81(33)	0.82(13)
168740	6871	90304	6.138	0.201	0.136	0.035	145	7630(81)	3.88(14)	1.82(2)	1.21(1)
168947			8.123	0.196	0.172	0.116		7555(185)	3.67(10)	1.28(30)	1.43(12)
170680	6944	90806	5.132	0.008	0.008	0.091	205	9840(248)	4.15(6)	0.83(23)	1.70(9)
175445		92884	7.792	0.110	0.055	0.108		8520(198)	3.96(10)	1.08(27)	1.53(11)
183324	7400	95793	5.795	0.084	0.051	0.083	90	8950(204)	4.13(4)	1.64(42)	1.32(17)
184779			8.940	0.224	0.187	0.000		7210(173)	3.63(21)	1.26(30)	1.43(12)
192640	7736	99770	4.934	0.154	0.099	0.016	80	7940(96)	3.95(18)	1.84(1)	1.22(1)
193256	7764C	100286	7.721	0.213	0.116	0.063	250	7740(94)	3.69(17)	1.08(30)	1.51(12)
193281	7764A	100288	6.557	0.190	0.098	0.111	95	8035(115)	3.54(4)	0.41(30)	1.79(12)
198160	7959	102962	5.663	0.189	0.108	0.022	200	7870(129)	3.99(9)	1.47(41)	1.36(16)
204041	8203	105819	6.456	0.161	0.092	0.026	65	7980(97)	3.97(8)	1.75(18)	1.25(7)
210111	8437	109306	6.377	0.203	0.136	0.000	55	7550(123)	3.84(15)	1.76(15)	1.23(6)
216847		113351	7.060	0.242	0.155	0.000		7355(78)	3.47(14)	0.93(24)	1.56(10)
221756	8947	116354	5.576	0.095	0.056	0.043	105	8510(188)	3.90(3)	1.16(16)	1.50(6)

Table 2. Calibrated values for the program stars using the models of Claret (1995); $t_{\rm rel}$ is the relative age ranging from zero for an object just arriving at the ZAMS to unity for a star at the TAMS; $\Delta\log g = \log g({\rm evol}) - \log g({\rm phot})$; $\log t_1$ and $\log t_2$ are the minimum and maximum ages derived from the error boxes.

HD	M [$M_\odot$]	$\Delta\log g$	$\log t$ [dex]	$\log t_1$ [dex]	$\log t_2$ [dex]	$t_{\rm rel}$
319	2.12(9)	+0.15	8.88	8.84	8.91	0.86(5)
6870	1.70(12)	+0.22	9.02	8.70	9.05	0.69(13)
7908	1.61(5)	+0.02	9.02	8.88	9.11	0.70(8)
11413	2.02(4)	+0.03	8.91	8.88	8.93	0.83(3)
13755	2.21(4)	+0.31	9.01	8.90	9.05	1.03(8)
15165	2.14(6)	+0.38	9.00	8.93	9.10	1.01(9)
23392	2.30(11)	−0.09	8.00	7.00	8.50	0.35(23)
24472	1.74(4)	+0.10	9.13	9.09	9.17	0.88(4)
30422	1.76(2)	+0.21	8.69	8.52	8.80	0.54(7)
31295	2.08(10)	+0.00	8.51	7.60	8.71	0.47(23)
35242	1.96(6)	+0.19	8.81	8.69	8.86	0.70(6)
54272	1.69(10)	+0.16	9.12	9.00	9.20	0.83(10)
74873	2.00(3)	+0.00	8.52	8.20	8.70	0.51(13)
75654	1.85(5)	+0.15	9.03	9.01	9.05	0.85(3)
81290	1.85(11)	−0.01	9.10	9.03	9.17	0.92(9)
83041	1.90(11)	+0.06	9.05	8.99	9.11	0.90(8)
83277	1.98(12)	+0.05	9.03	8.96	9.10	0.93(9)
84123	1.95(5)	+0.03	9.04	9.01	9.10	0.93(5)
87271	2.20(3)	+0.28	8.90	8.80	9.00	0.93(9)
90821	2.38(16)	+0.03	8.79	8.74	8.90	0.93(11)
91130	2.10(10)	+0.16	8.86	8.83	8.89	0.83(5)
101108	2.08(12)	−0.03	8.92	8.87	8.92	0.86(6)
102541	1.75(6)	−0.06	8.85	8.42	8.99	0.60(16)
105058	2.26(11)	−0.06	8.85	8.79	9.00	0.94(11)
105759	2.05(8)	+0.15	8.96	8.92	9.10	0.94(10)
106223	1.85(15)	+0.30	9.10	9.00	9.20	0.92(12)
107233	1.62(4)	+0.14	8.93	8.60	9.06	0.61(13)
109738	1.87(12)	+0.09	8.98	8.90	9.02	0.81(7)
110377	1.84(4)	+0.08	8.94	8.90	8.97	0.76(3)
110411	2.02(10)	+0.14	8.00	7.00	8.66	0.33(24)
111005	1.88(20)	+0.05	9.09	8.99	9.18	0.93(14)
111604	2.42(3)	−0.02	8.79	8.77	8.90	0.96(7)
120500	2.30(12)	−0.06	8.81	8.75	8.90	0.90(9)
120896	1.83(11)	+0.16	9.05	9.01	9.06	0.85(6)
125162	2.04(7)	+0.12	8.61	8.00	8.75	0.53(19)
125889	1.70(10)	+0.19	9.03	8.99	9.10	0.77(7)
130767	2.28(4)	+0.02	8.60	8.48	8.68	0.68(7)
142703	1.67(2)	+0.15	9.02	8.83	9.10	0.71(9)
142944	2.25(11)	+0.31	8.99	8.90	9.06	1.05(10)
149130	1.97(12)	+0.23	9.04	8.98	9.10	0.94(8)
153747	2.15(12)	+0.21	8.84	8.81	8.86	0.83(6)
154153	1.84(10)	+0.30	9.08	9.03	9.13	0.89(7)
156954	1.56(8)	+0.14	8.92	7.00	9.01	0.44(29)
168740	1.88(2)	+0.10	8.97	8.94	8.99	0.81(2)
168947	2.09(12)	+0.13	8.94	8.88	9.01	0.91(8)
170680	2.50(10)	−0.08	8.48	8.30	8.57	0.66(10)
175445	2.25(12)	−0.03	8.78	8.73	8.82	0.83(6)
183324	2.09(17)	+0.07	8.50	7.00	8.73	0.45(29)
184779	2.08(12)	+0.08	8.97	8.91	9.03	0.93(8)
192640	1.90(2)	+0.10	8.90	8.85	8.91	0.75(2)
193256	2.18(12)	+0.09	8.89	8.83	9.00	0.92(10)
193281	2.50(12)	+0.08	8.75	8.70	8.81	0.93(7)
198160	2.02(18)	−0.06	8.92	8.86	8.95	0.84(9)
204041	1.93(7)	+0.06	8.90	8.82	8.92	0.76(5)
210111	1.90(5)	+0.11	8.98	8.95	9.02	0.84(4)
216847	2.21(10)	+0.17	8.90	8.87	9.00	0.96(8)
221756	2.20(8)	+0.06	8.78	8.73	8.82	0.80(5)

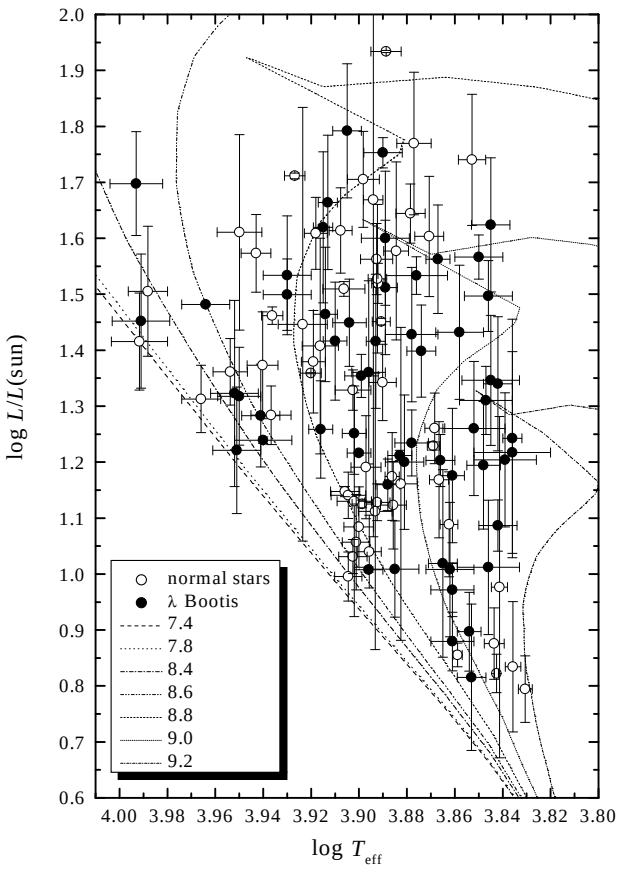

Figure 1. The sample of λ Boötis (filled circles) and normal-type (open circles) stars within a $\log {\rm L}_*/{\rm L}_\odot$ versus $\log T_{\rm eff}$ diagram. The isochrones (the different $\log t$ values are listed in the legend) were taken from Claret (1995).

Table 3. Normal-type stars selected as comparison.

HD	HIP	HD	HIP	HD	HIP
2262	2072	71297	41375	160613	86565
3003	2578	79439	45493	170642	90887
5382	4366	85364	48341	175638	92946
9919	7535	87696	49593	181296	95261
11636	8903	88824	50070	186689	97229
13041	9977	96113	54137	187642	97649
16555	12225	98058	55084	192425	99742
17943	13421	98353	55266	195050	100907
19107	14293	101107	56770	196078	101608
39060	27321	102124	57328	201184	104365
40136	28103	105211	59072	205835	106711
45320	30666	111968	62896	205852	106787
49434	32617	116706	65466	205924	106856
50241	32607	118232	66234	207235	107596
50277	33024	122405	68478	207958	108036
50506	31897	135379	74824	210300	109412
56405	35180	135559	74689	210739	109667
59037	36393	145631	79439	211356	109984
70574	41036	159561	86032	220061	115250

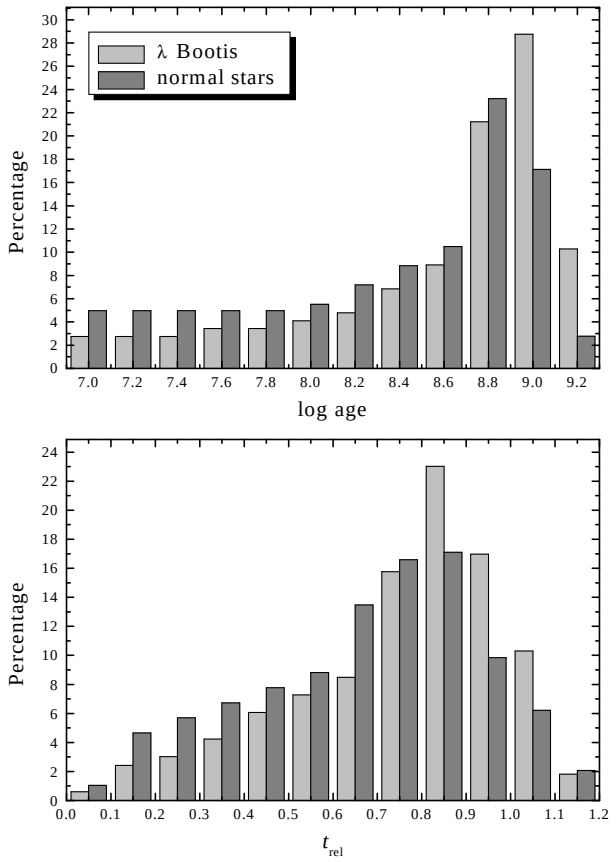

Figure 2. Histogram of the calibrated ages (upper panel) and relative ages for both samples (lower panel).

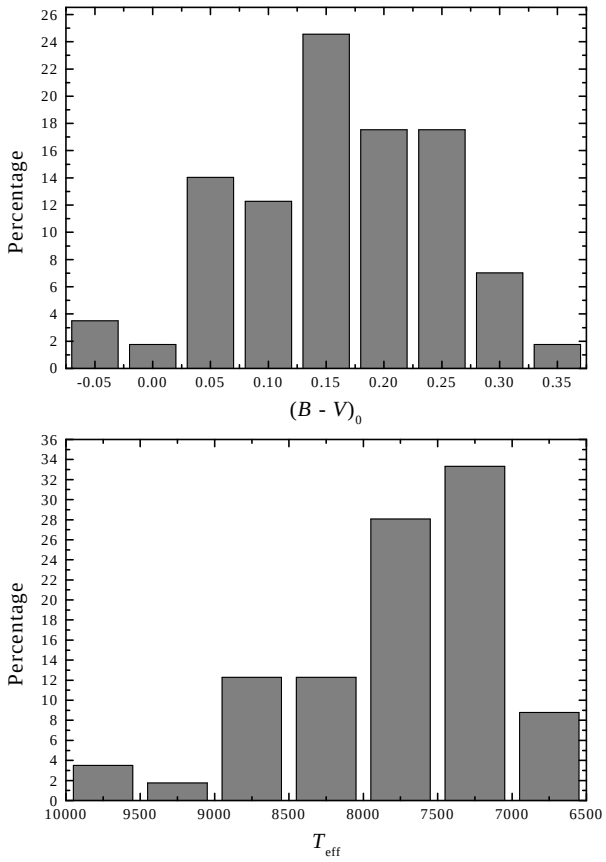

Figure 4. Histogram of $(B-V)_0$ values (upper panel) and the calibrated effective temperature (lower panel) for the sample of λ Boötis stars.

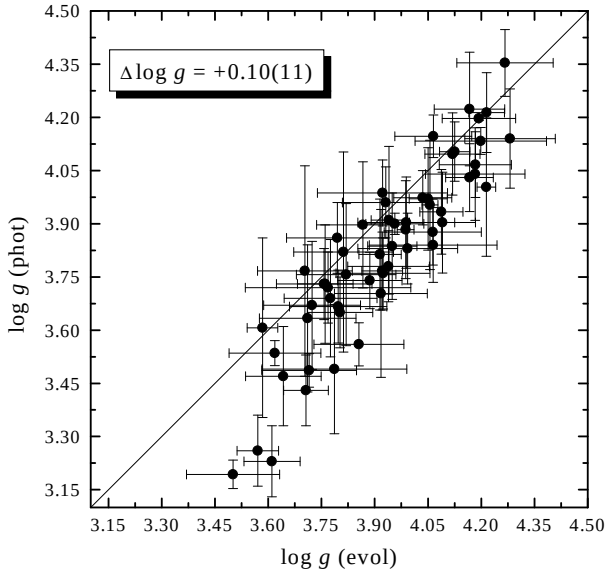

Figure 3. Surface gravities calibrated photometrically and calculated via the mass, luminosity and effective temperature; the mean difference $\Delta\log g = +0.10(11)$ is not significant.

3 A TEST SAMPLE OF NORMAL STARS

For comparison with the results obtained for the λ Boötis stars we generated a test sample of apparently normal dwarfs with the same effective temperatures. We limited the sample to luminosity class V objects for which photometric and Hipparcos measurements are available. Known spectroscopic binary systems were excluded. Then, only objects for which the spectral classifications published by Gray & Garrison (1987; 1989a,b) and Garrison & Gray (1994) agree within two temperature sub-classes with those by Abt & Morell (1995) have been considered. The final sample (see Table 3) has the same number of stars as the λ Boötis list. Special attention has been paid to the $(B-V)_0$ distribution of the test sample to ensure that it similar to that of the λ Boötis objects (Fig. 4, upper panel). Thus, the test sample represents luminosity class V stars in the solar neighbourhood, covering the same spectral range as the λ Boötis group.

All basic parameters were derived in exactly the same way as for the λ Boötis objects. All statistical significance levels presented in the following sections are based on several hypothesis tests (e.g. t-test; Rees 1987).

We have not explicitly listed the parameters of this sample but it is available in electronic form via anonymous ftp 130.79.128.5 or http://cdsweb.u-strasbg.fr/Abstract.html.

4 THE HERTZSPRUNG–RUSSELL DIAGRAM BASED ON HIPPARCOS AND PHOTOMETRIC DATA

Earlier investigations already concluded that the group of λ Boötis stars comprises the whole area between the ZAMS and TAMS. Only the interpretation of the evolutionary stage (PMS or post-MS) varied. In this work we have not investigated a possible PMS hypothesis as proposed by Paunzen (1997). Beside the arguments given in Bohlender et al. (1999) and Faraggiana & Bonifacio (1999) we would like to add a few more points. If we speculate that some of these stars are in a PMS phase then they would have ages of one Myr or even younger since they are in the 'right upper corner' of the Hertzsprung–Russell diagram (HRD hereafter) very close to the birth-line according to the models of Palla & Stahler (1993). So they should be very bright in the IR region and lie within the boundaries of star-forming regions or molecular clouds; neither implication has been verified so far (King 1994).

Figure 1 shows the HRD with the data taken from Table 1. The post-MS evolutionary isochrones are from Claret (1995). It is encouraging to see that no object lies below the ZAMS; that gives further confidence in the calibrations used.

To estimate the most probable age distribution of our program stars, we have used a moving average (Fig. 2). Such a method takes into account the errors of individual data as it counts all points (plus and minus the standard deviation) which lie in a certain bin (Rees 1987). From the histogram it is clear that the group of λ Boötis stars comprises evolutionary stages of the entire MS with a peak at $t_{\rm rel} \approx 0.85$ (about 1 Gyr). Taking the few candidates in the Orion OB1 association and NGC 2264, the percentage for very young objects ($\log t < 7.0$) would be approximately 5% which fits very well into the overall picture.

Since the distribution of the test sample (Fig. 2) agrees at a 99.9% significance level, the age distribution of the λ Boötis objects is *not* distinct from that of other luminosity class V objects in the same spectral domain within the solar neighbourhood. That is already a first hint that the mechanism behind the λ Boötis phenomenon operates only within very tight constraints, since only 2% of all stars are objects of the λ Boötis type.

Gray & Corbally (1998, 1999) made an extensive survey for λ Boötis stars in 24 open clusters and associations and found not a single candidate. The cluster ages range from 15 to 700 Myr. Therefore, only a few candidates in the Orion OB1 association and NGC 2264 remain. It seems that the star-formation process within open clusters does not favour the manifestation of the λ Boötis phenomenon.

Table 4 lists the 16 stars that we have in common with the papers of Iliev & Barzova (1995) and Paunzen (1997). For the calibration of effective temperatures they both used the method of Moon & Dworetsky (1985) within the Strömgren *uvbyβ* photometric system; Iliev & Barzova (1995) also derived the luminosities with this calibration whereas Paunzen (1997) took advantage of the Hipparcos data. For the calibration of mass and age, Iliev & Barzova (1995) interpolated between the evolutionary tracks given by Schaller et al. (1992), whereas Paunzen (1997) used the CESAM models by Morel (1997). As expected, there are star-to-star variations, but overall the parameters fit well. The effective temperatures from this work are in very good agreement with those of both references. The luminosities and thus the calibrated ages are in better agreement with those of Iliev & Barzova (1995).

As a further test of the calibrated values, we have calculated the surface gravity via the effective temperature, mass and luminosity. Figure 3 shows the correlation of the photometrically calibrated surface gravity $\log g$(phot) and the calculated one $\log g$(evol). The mean errors for both parameters are typically ± 0.1 dex. Although there is some indication of a systematic offset, the mean difference $\Delta \log g = \log g(\text{evol}) - \log g(\text{phot}) = +0.10(11)$ is not significant. A similar effect was already noticed by Iliev & Barzova (1995) whereas Faraggiana & Bonifacio (1999) reported an inconsistency between the position in the HRD and the $\log g$ values derived from Strömgren *uvbyβ* photometry using the calibration of Moon & Dworetsky (1985). We conclude that the photometric calibrations for the group of λ Boötis stars are valid, in contradiction to the results of Faraggiana & Bonifacio (1999).

Before making a detailed statistical analysis, we looked to see whether our sample exhibits an apparent bias. Figure 4 shows that the sample includes significantly more cooler objects (70%) with effective temperatures lower than 8000 K. However, there is no observational bias from classification-resolution spectroscopy since the spectroscopic survey for new members included many more hotter- than cooler-type objects (Gray & Corbally 1999, Paunzen 2001). That fact could be interpreted as a manifestation of the working mechanism itself, or it could be due to the method used in this very limited spectral range. It is well known that at cooler temperatures (spectral domain A5 to F2), even a moderate metal-weakness can be detected at classification resolution since the overall metallic-line spectrum is much richer than for an A0-type object. However, we are not able to decide whether the distribution of the λ Boötis sample is due to a bias within the observational technique or due to the phenomenon itself.

Figure 5 shows the averaged effective temperatures, masses and projected rotational velocities for each age bin. The mean effective temperature is rather constant up to $t_{\rm rel} \approx 0.5$ with values between 8300 K to 8800 K. It then decreases linearly almost to 7000 K for the most evolved objects. The mean masses are constant within the error bars at about 1.9 $M_\odot$ for $t_{\rm rel} < 0.75$ and then increase to almost 2.2 $M_\odot$. Most interesting is the non-existence of a correlation of the projected rotational velocity with age. The mean value for the whole range is about 120 km s^{-1}. If we compare these results with those of our test sample, we find several differences as well as similarities:

- The trends for the effective temperature and mass are identical. However, the λ Boötis objects seem to have lower temperatures as well as masses for $t_{\rm rel} > 0.8$
- The $v \sin i$ distributions are identical within 1σ with a slightly higher scatter for the λ Boötis group ($\overline{\sigma}_{LB} = 19$ km s^{-1} and $\overline{\sigma}_{Nor} = 15$ km s^{-1})

Overall, there is no obvious distinction between the two samples.

Gray (1988) reported that several λ Boötis stars exhibit peculiar hydrogen-line profiles with weak cores and broad

Table 4. Comparison of the calibrated stellar parameters from this work (columns TW), Iliev & Barzova (1995; columns IL95) and Paunzen (1997; columns PA97).

HD	$\log T_{\rm eff}$			$\log L_*/L_\odot$			M			$\log t$			$t_{\rm rel}$	
	TW	IL95 ±0.02	PA97 ±0.02	TW	IL95 ±0.01	PA97	TW	IL95 ±0.2	PA97 ±0.1	TW	IL95 ±0.05	PA97 ±0.05	TW	IL95
319	3.904(7)	3.92	3.91	1.45(8)	1.53	1.34(5)	2.12(9)	2.2	2.0	8.88	8.81	8.76	0.86(5)	0.77
11413	3.899(4)	3.91	3.91	1.35(4)	1.41	1.28(4)	2.02(4)	2.1	1.9	8.91	8.87	8.82	0.83(3)	0.71
30422	3.896(6)	3.91	3.90	1.01(1)	1.03	0.96(3)	1.76(2)	1.8	1.8	8.69	8.58	7.00	0.54(7)	0.23
31295	3.950(9)	3.96	3.95	1.32(9)	1.40	1.20(3)	2.08(10)	2.2	2.0	8.51	8.54	7.00	0.47(23)	0.38
107233	3.861(9)	3.86	3.87	0.88(5)	0.94	0.80(5)	1.62(4)	1.6	1.6	8.93	9.04	7.00	0.61(13)	0.52
110411	3.951(10)	3.96	3.94	1.22(11)	1.30	1.09(3)	2.02(10)	2.1	1.9	8.00	8.30	7.00	0.33(24)	0.19
125162	3.935(5)	3.95	3.94	1.28(9)	1.38	1.20(1)	2.04(7)	2.1	2.0	8.61	8.58	7.20	0.53(19)	0.40
142703	3.868(9)	3.87	3.86	0.97(5)	1.00	0.93(3)	1.67(2)	1.7	1.7	9.02	9.02	8.50	0.71(9)	0.56
183324	3.950(5)	3.97	3.96	1.32(17)	1.51	1.20(4)	2.09(17)	2.3	2.1	8.50	8.52	7.00	0.45(29)	0.42
192640	3.903(2)	3.91	3.90	1.22(1)	1.23	1.16(2)	1.90(2)	1.9	1.9	8.90	8.85	8.65	0.75(2)	0.54
193256	3.894(9)	3.92	3.90	1.51(12)	1.48	1.50(27)	2.18(12)	2.1	2.2	8.89	8.86	8.79	0.92(10)	0.78
193281	3.907(8)	3.92	3.91	1.79(12)	1.81	1.96(27)	2.50(12)	2.5	2.5	8.75	8.72	8.84	0.93(7)	0.91
198160	3.907(13)	3.90	3.90	1.36(16)	1.24	1.37(7)	2.02(18)	1.9	2.0	8.92	8.86	8.77	0.84(9)	0.58
204041	3.906(6)	3.91	3.91	1.25(7)	1.21	1.20(7)	1.93(7)	1.9	1.9	8.90	8.81	8.57	0.76(5)	0.48
210111	3.888(3)	3.89	3.88	1.23(6)	1.30	1.16(5)	1.90(5)	2.0	1.8	8.98	8.94	8.84	0.84(4)	0.69
221756	3.931(9)	3.96	3.96	1.50(6)	1.67	1.41(4)	2.20(8)	2.4	2.2	8.78	8.65	8.10	0.80(5)	0.68

but often shallow wings. Iliev & Barzova (1993) examined the peculiar profiles of four objects. They were able to fit those profiles with two models having different temperatures (hotter for the wings by approximately 400 K) and concluded that it is a sign of circumstellar material around the objects. Faraggiana & Bonifacio (1999) interpret the peculiar profiles as an indication of undetected spectroscopic-binary systems in which two stars with solar abundances but different stellar parameters mimic one apparently metal-weak object. The classification of the hydrogen-line profiles for 19 stars were taken from Gray & Corbally (1993) and Paunzen & Gray (1997). For our sample we find only two objects (HD 30422 and HD 107233) with peculiar profiles among the younger objects ($t_{\rm rel} < 0.66$) but seven with normal ones. The picture for the older objects is just the opposite: there are only two objects (HD 90821 and HD 120500) with normal profiles but nine with peculiar ones.

Several attempts were made to detect signs of circumstellar lines in the optical domain (Andrillat, Jaschek & Jaschek 1995; Hauck, Ballereau & Chauville 1995, 1998; Holweger, Hempel & Kamp 1999). From our list, sixteen objects were investigated but only three objects have positive detections: HD 11413, HD 193256 and HD 198160 (Holweger et al. 1999). These stars are rather evolved ($t_{\rm rel} = 0.83$, 0.92 and 0.84, respectively) but owing to the poor number statistics, any conclusion about the significance has to be treated with caution.

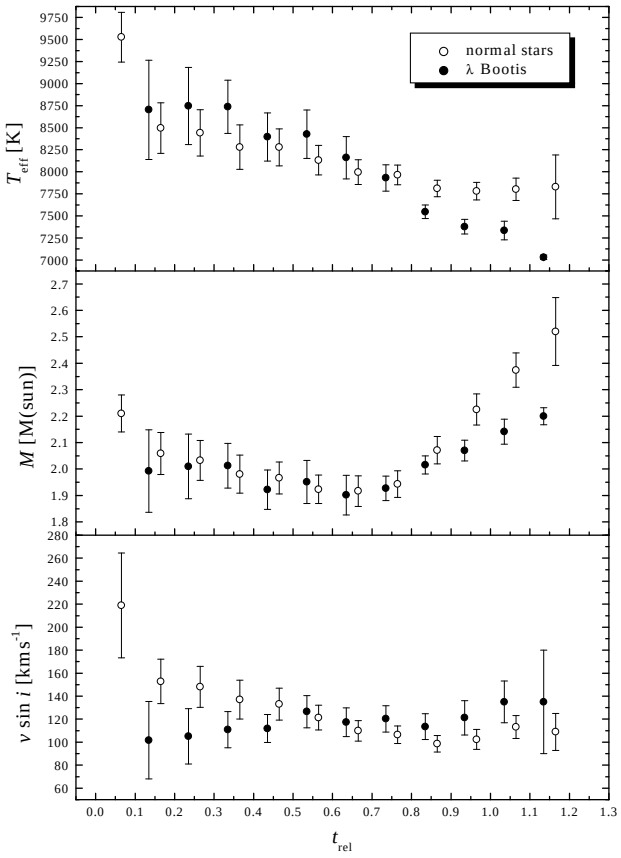

Figure 5. Correlation found for the effective temperature (lower panel) and mass (middle panel) with the relative age; no correlation is detected with the projected rotational velocity (upper panel). The λ Boötis (filled circles) and normal-type (open circles) stars are binned with respect to their relative age.

5 THE ABUNDANCE PATTERN OF λ BOÖTIS STARS

Since the first detailed abundance analysis in the late eighties, there has been a question as to whether a unique abundance pattern exists for the λ Boötis group. Most of the proposed candidates for membership have been found by classification-resolution spectroscopy (typically 40 Å mm^{-1} to 120 Å mm^{-1}). In the classical photographic domain (3800 to 4600 Å) spectral lines of Ca, Mg, Fe and Ti are the main contributors to the overall appearance of the metallic-line spectrum. Gray (1988) defined the membership of the class in terms of a weak Ca K and metallic-line spectrum compared to the temperature classification of the hydrogen lines.

Paunzen et al. (1999a) and Kamp et al. (2001) already investigated the behaviour of the lights elements C, N, O and S for a statistically significant number of members:

- The star-to-star scatter for the abundances of C, N, O and S is much smaller than that for heavier elements
- The abundances of C, N, O and S are not strictly solar but range from −0.8 dex to +0.2 dex compared to the Sun
- Fe-peak elements are always more underabundant

Table 5. Abundances from the literature for our program stars. Different values for a single element were added and a mean was calculated. All values are given with respect to the Sun as: $[X] = \log X - \log X_{\odot}$. In parentheses are the estimated errors of the means or the individual error taken from the relevant reference.

HD	C	N	O	Na	Mg	Al	Si	S	Ca
319	−0.16(15)	–	+0.22(10)	+1.00(10)	−0.73 (5)	−0.58(20)	−0.45(10)	–	−0.68(20)
11413	−0.15(15)	–	−0.10(10)	–	−1.18(20)	–	−0.20(20)	–	−0.74(30)
15165	+0.00(30)	–	−0.30(30)	+0.00(30)	−1.50(30)	–	−0.90(30)	+0.00(30)	−1.00(30)
31295	−0.17(15)	−0.24(15)	−0.29(15)	−0.52(20)	−1.15(20)	–	−0.95(20)	−0.16(20)	−0.90(20)
74873	+0.60(10)	–	−0.10(30)	+0.50(30)	−0.90(10)	−1.10(30)	–	–	−1.00(30)
75654	−0.44(10)	+0.00(15)	+0.14(10)	–	−0.52(18)	–	–	−0.10(15)	−0.84(15)
84123	−0.01(24)	+0.00(30)	−0.30(20)	−0.55(40)	−0.76(20)	–	−0.75(20)	−0.50(10)	−0.58(20)
91130	+0.20(30)	+0.30(15)	+0.11(30)	–	−0.63 (6)	–	−0.45 (7)	+0.18(15)	−3.00(15)
101108	+0.10(10)	–	–	–	−0.30(20)	−0.90(30)	−0.50(30)	–	−0.60(10)
106223	+0.30(10)	–	–	–	−1.40(30)	−2.10(30)	−1.70(30)	–	−1.59(10)
107233	−0.30(30)	–	–	–	−0.80(20)	−2.20(30)	–	–	−1.40(10)
110411	+0.10(20)	+0.30(30)	–	–	−0.50(10)	–	−0.30(30)	–	−0.84(20)
111604	−0.25 (5)	–	–	+0.47(15)	−0.98 (5)	–	−0.85(30)	–	–
120500	+0.20(20)	+0.00(15)	−0.09(15)	+0.32(30)	−0.23 (7)	–	−0.95 (5)	−0.13(15)	−0.30(15)
125162	−0.34(20)	−0.12(15)	−0.22(20)	−1.30(15)	−2.00(20)	–	−1.00(20)	−0.45(15)	−1.98(15)
142703	−0.28(20)	−0.50(15)	−0.19(10)	–	−1.20(20)	–	–	−0.53(15)	−1.20(10)
168740	−0.42(10)	–	−0.03(10)	–	−0.90(10)	–	–	–	−0.60(20)
170680	−0.06(10)	−0.07(10)	–	–	−0.20(20)	–	–	–	–
183324	+0.11(20)	−0.03(30)	−0.10(30)	+0.10(30)	−1.73(20)	−1.50(30)	−1.10(20)	−0.13(15)	−1.32(30)
192640	−0.19(20)	−0.22(15)	−0.32(30)	−1.10(20)	−1.62(20)	–	−1.00(30)	−0.31(15)	−1.35(20)
193256	−0.45(20)	–	−0.23(10)	+0.90(30)	−0.15(20)	–	+0.00(30)	–	−0.51(30)
193281	−0.49(20)	+0.30(15)	−0.05(10)	+1.00(20)	−0.08(10)	–	–	+0.14(15)	−0.68(20)
198160	−0.18(30)	–	−0.18(10)	+0.30(20)	−0.13(10)	–	−0.20(20)	–	−0.67(30)
204041	−0.58(20)	−0.05(15)	−0.42(20)	+0.36(20)	−1.04(20)	−0.93(20)	−0.63(20)	+0.07(20)	−0.98(20)
210111	−0.23(10)	–	−0.20(10)	+0.60(10)	−1.00(12)	−0.52(20)	−0.65(10)	–	−0.96(20)
221756	+0.00(20)	+0.20(15)	+0.17(20)	+1.17(20)	−0.70(20)	–	−1.00(20)	+0.06(15)	−0.49(20)

	Sc	Ti	Mn	Cr	Fe	Ni	Sr	Y	Ba
319	−1.10(20)	−0.75(20)	–	−0.40(20)	−0.64(20)	–	−0.35(30)	–	−0.25(20)
11413	−1.10(30)	−1.40(20)	–	−1.20(20)	−1.43(20)	–	−1.50(20)	–	−0.90(20)
15165	−1.40(30)	−0.50(30)	–	−0.90(30)	−1.60(30)	−1.00(30)	−0.80(30)	–	–
31295	−0.90(30)	−0.96(20)	–	−0.75(20)	−1.07(20)	−0.50(20)	−1.51(20)	–	−0.45(20)
74873	−0.40(30)	−0.90(10)	–	−0.30(20)	−0.70(10)	−0.20(30)	−0.90(40)	–	–
75654	–	−1.01(29)	−1.00(42)	−1.10(30)	−1.08(14)	–	–	–	–
84123	−0.90(31)	−0.86(10)	−0.84(20)	−0.85(30)	−0.72(20)	−0.74(30)	−0.50(30)	−0.55(13)	−0.60(20)
91130	–	−0.64 (8)	–	−0.48 (3)	−1.16 (8)	–	–	–	–
101108	−0.60(40)	−0.20(20)	−0.40(20)	−0.60(10)	−0.70(10)	−0.30(10)	−0.70(40)	+0.00(40)	−0.70(30)
106223	−1.10(30)	−1.02(10)	−1.70(10)	−1.34(20)	−1.60(10)	−0.97(20)	−1.70(30)	−0.50(30)	−1.60(20)
107233	−1.70(30)	−1.34(30)	−1.30(20)	−1.28(30)	−1.38(21)	–	−1.30(30)	−0.90(30)	–
110411	−1.10(30)	−0.90(10)	–	–	−1.07(20)	–	−1.10(20)	–	–
111604	–	–	–	−1.07(30)	−1.08 (4)	–	–	–	–
120500	–	–	–	–	−0.67 (6)	–	–	–	–
125162	−0.70(20)	−2.01(20)	–	−1.00(20)	−1.98(20)	−1.20(20)	−2.10(15)	–	−0.90(20)
142703	−1.50(30)	−1.27(10)	–	−1.40(10)	−1.32(12)	−0.90(20)	−1.20(30)	–	−1.50(30)
168740	−1.10(30)	−0.88(10)	–	−1.10(10)	−0.88(10)	–	−1.00(30)	–	−0.50(30)
170680	–	−0.40(10)	–	−0.40(30)	−0.50(10)	–	–	–	–
183324	−1.46(40)	−1.42(20)	–	−1.38(20)	−1.50(30)	–	−2.00(30)	–	−0.67(20)
192640	−1.15(20)	−1.33(20)	−2.00(20)	−1.65(20)	−1.63(20)	−0.60(20)	−1.49(30)	–	−1.03(20)
193256	−0.90(40)	−0.30(30)	–	−1.00(30)	−0.90(30)	–	−0.50(30)	–	−0.88(50)
193281	–	−0.36(20)	–	−0.20(20)	−0.93(20)	–	−0.10(20)	–	−0.54(20)
198160	–	−0.50(20)	–	−0.90(20)	−0.78(30)	–	−1.30(30)	–	−0.98(30)
204041	−1.03(40)	−1.21(20)	–	−0.72(30)	−0.87(20)	−0.40(20)	–	–	−0.09(20)
210111	−1.30(20)	−1.05(20)	–	−1.18(20)	−0.89(20)	–	+0.45(20)	–	−0.20(20)
221756	−0.60(20)	−0.50(20)	–	−0.50(20)	−0.59(30)	–	–	–	−0.15(30)

Heiter (2002) and Heiter et al. (2002) tried to shed more light on the abundance pattern in the context of the theories proposed. They used mean values for a sample of 34 stars (not all elements' abundances were determined for all objects) and concluded:

- The iron-peak elements from Sc to Fe as well as Mg, Si, Ca, Sr and Ba are underabundant by 1 dex compared to the Sun
- Al is slightly more depleted whereas Ni, Y and Zr are slightly less depleted

Table 6. Kinematic data from the Hipparcos database for the program stars. In parentheses are the errors in the final digits of the corresponding quantity.

HD	π [mas]	d [pc]	μ_α [mas yr^{-1}]	μ_δ [mas yr^{-1}]	RV [km s^{-1}]	U [km s^{-1}]	V [km s^{-1}]	W [km s^{-1}]
319	12.45(0.74)	80(5)	+70.01(0.94)	−34.71(0.41)	−10.7(9.9)	−18.1(1.8)	−25.5(1.8)	+4.9(9.7)
6870	10.30(0.61)	97(6)	+120.99(0.51)	−12.65(0.59)	+12.4(3.0)	−39.2(2.6)	−41.7(2.8)	−0.3(2.3)
7908	11.41(0.98)	88(8)	−5.54(1.04)	−37.51(0.50)	+13.2(3.0)	+9.2(1.0)	−11.3(1.1)	−14.5(3.0)
11413	13.37(0.64)	75(4)	−47.97(0.51)	−4.30(0.57)	+7.2(5.6)	+14.3(0.8)	+6.5(2.4)	−9.8(5.1)
15165	8.51(0.89)	118(12)	+35.50(1.10)	−11.70(0.74)	+33.5(2.1)	−32.4(1.8)	−8.6(1.4)	−20.8(2.1)
30422	17.40(0.68)	57(2)	−4.04(0.48)	+18.19(0.60)	+16.5(3.5)	−12.4(1.8)	−6.4(2.1)	−10.2(2.2)
31295	27.04(0.94)	37(1)	+40.08(1.04)	−128.37(0.65)	+12.9(1.7)	−6.0(1.6)	−23.9(0.7)	−10.8(0.8)
35242	13.32(0.98)	75(6)	−30.42(0.99)	+16.63(0.63)	+9.0(3.0)	−9.7(2.7)	+8.0(1.1)	−8.7(1.2)
74873	16.38(1.16)	61(4)	−65.20(1.25)	−51.06(0.70)	+23.3(3.0)	−23.0(2.4)	−22.9(1.4)	−7.9(2.1)
75654	12.82(0.58)	78(4)	−63.91(0.42)	+41.13(0.49)	+9.4(1.1)	−28.0(0.8)	−5.3(1.2)	−8.2(0.9)
84123	9.09(0.90)	110(11)	−20.74(1.11)	−86.15(0.43)	+16.3(3.0)	−16.0(2.3)	−45.5(4.4)	+8.4(2.3)
87271	6.80(0.88)	147(19)	+3.33(0.86)	+5.01(0.49)	+0.1(3.0)	+0.4(1.5)	+3.3(1.5)	+2.5(2.3)
91130	13.33(0.76)	75(4)	+17.10(0.60)	+6.89(0.42)	−14.5(3.0)	+11.6(1.5)	+5.6(0.4)	−9.4(2.6)
105058	5.32(1.04)	188(37)	−9.80(0.84)	+0.66(0.81)	−7.2(3.0)	−5.5(1.9)	−5.3(1.3)	−8.3(2.8)
106223	9.10(0.86)	110(10)	−67.32(1.04)	+19.29(0.55)	−15.4(3.7)	−32.8(2.9)	−7.3(1.9)	−20.9(3.7)
110377	14.60(0.80)	68(4)	−106.08(0.78)	+0.71(0.48)	+3.0(8.5)	−29.0(1.9)	−18.7(2.5)	+1.6(8.1)
110411	27.10(0.82)	37(1)	+82.62(0.80)	−89.51(0.48)	−12.7(11.5)	+18.7(1.5)	− 1.6(3.1)	−16.2(11.0)
111005	5.75(1.01)	174(31)	−43.12(0.86)	−6.92(0.58)	+0.6(3.0)	−27.1(5.3)	−23.6(3.1)	−2.6(3.5)
111604	8.43(0.73)	119(10)	−88.59(0.67)	+21.83(0.56)	−17.1(4.7)	−46.7(3.7)	−19.4(2.4)	−19.3(4.8)
120500	6.97(0.90)	143(19)	−26.63(0.70)	+10.97(0.68)	+7.1(3.3)	−15.0(2.4)	−6.4(1.9)	+13.0(2.9)
120896	4.87(1.15)	205(48)	−18.65(1.14)	+3.00(0.78)	−24.4(3.0)	−25.0(3.7)	−5.5(3.0)	−16.7(2.6)
125162	33.58(0.61)	30(1)	−187.42(0.52)	+159.01(0.43)	−0.3(4.0)	−34.6(0.5)	−5.1(1.7)	−2.6(3.6)
130767	7.82(0.78)	128(13)	−46.63(0.69)	−6.87(0.62)	−14.0(3.0)	−20.5(2.0)	−24.4(2.1)	−0.7(3.0)
142703	18.89(0.78)	53(2)	+71.62(0.83)	−305.20(0.67)	+15.9(5.4)	+23.5(4.8)	+4.0(0.7)	−9.2(2.6)
153747	5.32(0.98)	188(35)	+6.55(0.99)	+14.08(0.68)	−6.3(0.5)	−3.2(1.1)	+14.6(1.8)	+2.8(1.9)
154153	15.16(1.11)	66(5)	+11.40(0.90)	+25.04(0.61)	−32.6(3.0)	−28.6(2.9)	+17.5(1.0)	+3.0(0.5)
168740	14.03(0.69)	71(4)	+0.57(0.59)	−101.87(0.49)	−21.1(3.0)	−36.3(2.6)	−17.5(1.9)	−2.8(1.2)
170680	15.30(0.81)	65(3)	−6.98(0.84)	−21.43(0.64)	−34.6(3.5)	−31.8(3.4)	−15.2(0.9)	+1.3(0.4)
183324	16.95(0.87)	59(3)	−0.51(0.72)	−33.35(0.43)	+12.0(3.0)	+14.1(2.3)	+0.7(1.9)	−5.7(0.5)
192640	24.37(0.55)	41(1)	+69.22(0.46)	+68.67(0.45)	−18.1(1.1)	−22.7(0.4)	−12.4(1.1)	−4.2(0.3)
193281	4.58(1.59)	218(76)	−4.32(1.54)	−0.75(1.07)	+2.0(2.7)	+4.2(2.5)	−1.0(1.3)	+2.5(2.3)
198160	13.67(1.16)	73(6)	+83.04(0.86)	−49.38(0.92)	−16.0(3.0)	−34.9(2.4)	−8.6(2.3)	−9.3(2.5)
204041	11.46(0.99)	87(8)	+50.00(1.18)	+13.84(0.77)	−15.1(26.7)	−25.1(13.3)	−6.7(17.9)	−3.4(14.8)
210111	12.70(0.89)	79(6)	+13.66(0.86)	+24.90(0.48)	−4.4(1.1)	−8.5(0.7)	+7.7(0.7)	+0.7(0.9)
216847	6.76(0.67)	148(15)	+16.85(0.43)	+12.33(0.40)	−3.0(1.4)	−12.6(1.2)	+5.3(0.7)	−6.1(1.5)
221756	13.97(0.63)	72(3)	−17.71(0.45)	−45.77(0.42)	+13.4(0.5)	+7.7(0.5)	+10.9(0.6)	−16.7(0.6)

- The mean abundance of Na is solar, but the star-to-star scatter is about ±1 dex
- The star-to-star scatter is twice as large as for a comparable sample of normal stars

Otherwise they find no, or only a poor, correlation of individual abundances with astrophysical parameters such as the effective temperature, surface gravity, projected rotational velocity, age and pulsational period.

We have used the individual abundances published by Venn & Lambert (1990), Stürenburg (1993), Holweger & Rentzsch-Holm (1995), Chernyshova et al. (1998), Heiter et al. (1998), Paunzen et al. (1999a,b), Kamp et al. (2001), Solano et al. (2001), Heiter (2002) and Andrievsky et al. (2002) for members of the λ Boötis group. The individual values were weighted according to the errors listed in the references. For our further analysis we have used only objects for which an abundance of carbon or oxygen is available, since those are key elements for the definition of the λ Boötis group.

Values for stars of superficially normal type were taken from Adelman (1991, 1994, 1996), Adelman et al. (1991, 1997), Hill & Landstreet (1993), Hill (1995), Caliskan & Adelman (1997) and Varenne & Monier (1999).

Let us recall that the membership of an object in the λ Boötis group is mainly based on spectroscopy at classification resolution. The only other approach is the definition of membership criteria in the UV region (Solano & Paunzen 1999). No reference in the literature was found which describes membership criteria based on detailed abundance analysis in the optical region. If we compare the status of other chemically peculiar stars of the upper main sequence then a similar situation is evident (Wolff 1983; Cowley 1995). Objects have been classified as being chemically peculiar but their individual elemental abundances differ widely. No attempt has so far been made to define the membership of the classical CP stars to a sub-class by detailed abundances alone (Preston 1974).

The λ Boötis group is unusual in this respect since it shows strong underabundances, not found for any other group, of most heavier elements. The only exceptions are intermediate and true Population II-type objects and

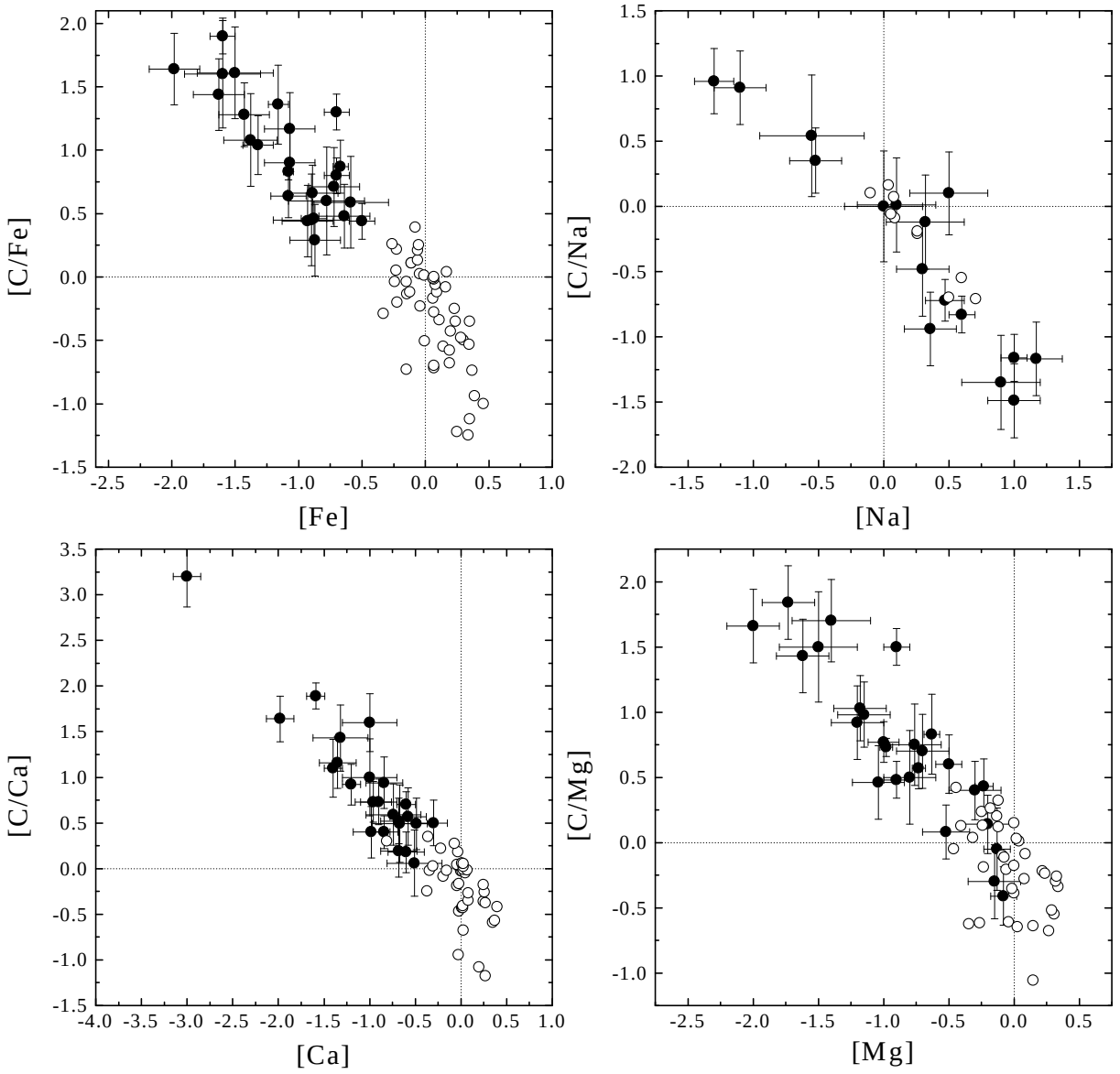

Figure 6. Abundance ratios for the λ Boötis stars (filled circles); open circles denote normal-type stars from the literature.

field blue stragglers, post-AGB and F-weak stars (Gray 1988, 1989; Jaschek, Andrillat & Jaschek 1989; Andrievsky, Chernyshova & Ivashchenko 1995; van Winckel, Waelkens & Waters 1995). Objects with very low surface gravities (post-AGB and Population II-type objects) are easily distinguished even at classification resolution and will not be considered in the following discussion. For the other groups the underabundances of the Fe-peak elements are rather moderate. But, more importantly, the abundances of the light elements C, N, O and S scale just like those of the heavier elements. We have therefore chosen to use [C/Z] versus [Z] diagrams ([O/Z], [N/Z] and [S/Z] behave analogously) in order to investigate the behaviour of the group of λ Boötis stars. The field blue stragglers, intermediate Population II and F-weak types of stars all fall in the area around $[C/Z] \approx 0$ in these diagrams.

Figure 6 shows such diagrams for the elements Fe, Na, Ca and Mg for the stars on our program as well as for those of superficially normal types. From this Figure we are able to conclude:

- All program stars are Population I-type objects with $[C/Fe] \gg 0$
- The λ Boötis stars exhibit iron abundances that are significantly lower than those found for the superficially normal stars
- There is a large overlap for all other heavier elements

Cowley et al. (1982) have proposed that λ Boötis-type and other weak-line stars may arise from small (≈ 0.3 dex) abundance fluctuations in the interstellar medium. That might be true for a small fraction of the objects, but underabundances up to a factor of 100 can not be explained without

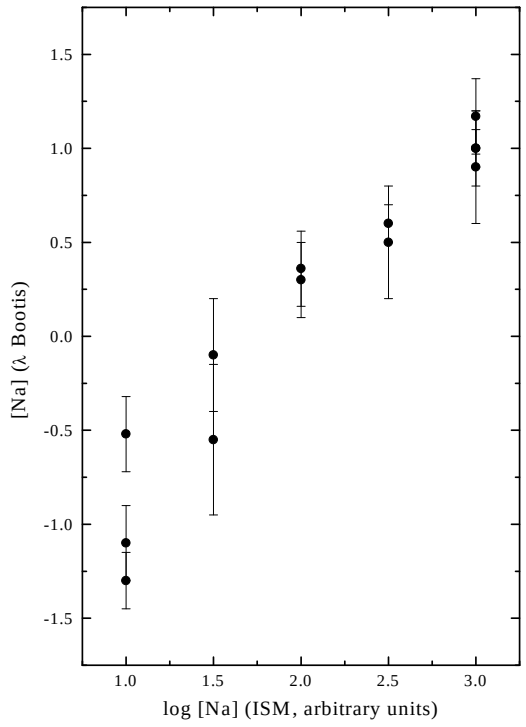

Figure 7. Correlation between the sodium abundances for 13 λ Boötis stars and the values, taken from Welsh et al. (1998), for the surrounding environment. The latter values are scaled in three steps (a value of three denotes the highest density).

some other mechanism such as diffusion, accretion or mass-loss.

A very intriguing fact is that eight program stars exhibit magnesium abundances which range from −0.52 to −0.13 dex, which seems to contradict the classification based on moderate-resolution spectroscopy. One of the most important classification criterion is the moderate to extreme weakness of the Mg II 4481 Å line (Gray 1988). What can actually cause that discrepancy? Slettebak, Kuzma & Collins (1980) have shown that the equivalent width of the line decreases with increasing rotation for models later than A0. The same fact was also described by Abt & Morrell (1995). A much stronger effect was found for Hγ. That means that a rapidly rotating star will be classified much later according to Hγ than on the basis of Mg II 4481 Å. Taking a rapidly rotating A5 type star one would classify it as hF1mA7 or metal-weak. However, the three objects with the highest magnesium abundances of our sample are indeed the fastest rotators: HD 193256 (250 $\mathrm{km\,s^{-1}}$; −0.15 dex), HD 170680 (205 $\mathrm{km\,s^{-1}}$; −0.20 dex) and HD 198160 (200 $\mathrm{km\,s^{-1}}$; −0.13 dex). But there is no overall correlation for the whole sample, i.e. fast rotators do also exhibit rather strong underabundances (e.g. HD 111604) and vice versa. Otherwise the fast rotators are not outstanding in any respect.

One observational fact is the wide range of abundances (−1.3 to +1.2 dex) for sodium (Table 5 and Fig. 6) first indicated in the work of Stürenburg (1993). In the recent literature no explanation of the variability has been given. Sodium is the only element for which such a behaviour has been detected so far. Furthermore, predictions for that element have not been discussed so far within any proposed theory (Turcotte & Charbonneau 1993). In an effort to shed some light on the subject, we have investigated whether a correlation can be found between the individual sodium abundances and the density of sodium in the surrounding interstellar medium. Welsh, Crifo & Lallement (1998) published the local distribution of interstellar Na I within 250 pc of the Sun. They used all published absorption densities and the distances derived from the Hipparcos satellite. The densities were scaled in three steps (a value of three denotes the highest density) and plotted for different Galactic coordinates and distances from the Sun. We have selected members of the λ Boötis group whose sodium abundances are known and for which nearby data points are available in the maps of Welsh et al. (1998). We have also checked more recent references such as Sfeir et al. (1999) and Vergely et al. (2001) which give essentially the same results. In total, thirteen objects fulfill the requirements: HD 319, HD 31295, HD 74873, HD 84123, HD 125162, HD 183324, HD 192640, HD 193256, HD 193281, HD 198160, HD 204041, HD 210111 and HD 221756.

We have to emphasize that not a single sodium abundance for the line of sight to any λ Boötis star has yet been measured. Bohlender et al. (1999) reported a few detections of such features, e.g. for HD 319, HD 192640 and HD 221756, but they did not derive quantitative densities or abundances.

Figure 7 shows the correlation of the individual sodium abundances with the absorption densities for the local interstellar medium (ISM hereafter). Since there is a linear correlation visible it suggests that there is an interaction (e.g. accretion) between the stars and their environments at some stage of stellar evolution. The correlation does not reflect any age dependency, since objects are included with $0.33 < t_{\mathrm{rel}} < 1.01$. This rather small sample is reasonably representative of the whole sample of program stars in terms of its distribution in t_{rel} and effective temperature. Unfortunately it is not possible to include any data for superficially normal objects in Fig. 7 since no sodium abundances for bright field stars are available. The only data are those published by Varenne & Monier (1999; Fig. 6) for members of the Hyades.

From our current analysis two main questions arise for the λ Boötis phenomenon: How many mechanisms are involved? What are the observational constraints? It is clear that there is one mechanism which produces the observed pattern throughout the whole MS lifetime for stars between late B and early F types. We are not able to decide if it is 'internal' or 'external' but we have some hints about it. It is highly improbable that one mechanism works for early evolutionary stages and an independent second one at very late stages producing the same absolute abundance pattern. That seems to be supported by the non-existence of a correlation between the iron abundance and age (Fig. 8). The abundance of sodium for the stellar atmosphere is correlated with that of the local ISM. There are two possible explanations for that: 1) the atmospheric abundance resembles the one from the cloud in which the star was born, or 2) it currently interacts with the local ISM. If we believe in the first interpretation then all other abundances ought also

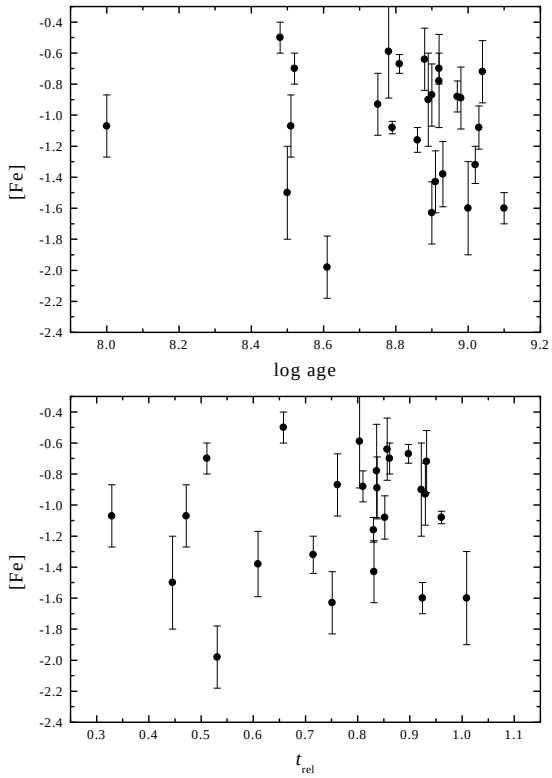

Figure 8. No correlation is found between iron abundance and age.

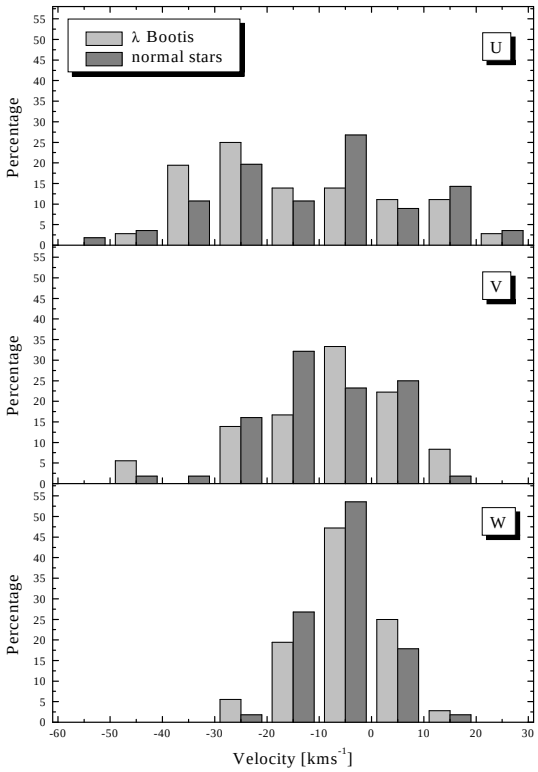

Figure 9. The histograms of the Galactic space-velocity components (U, V and W) for the λ Boötis and normal-type samples. The distributions agree at significance levels of 72% (U), 74% (V) and 97% (W).

to resemble those in the local ISM. That seems not to be the case, since many other 'normal' stars located within the same ISM clouds show no significant elemental underabundances at all. So we are left with the picture of an interaction between the star and its environment.

6 THE SPACE MOTIONS OF λ BOÖTIS STARS

In order to study the kinematics of nearby stars, one needs to calculate the Galactic space-velocity components (U, V and W), given the star's proper motion, parallax (both listed in the Hipparcos catalogue) and radial velocity. Here, the formulae and error propagation are taken from the Hipparcos documentation as well as from Johnson & Soderblom (1987).

It was chosen to calculate heliocentric Galactic velocity components, which can easily be corrected for the solar motion. A right-handed coordinate system for U, V and W was used, so they are positive in the directions of the Galactic centre, Galactic rotation and the North Galactic Pole. The 'standard solar motion' in this system would be (+10.4, +14.8, +7.3) taken from Mihalas & Routly (1968).

The authors followed the approach of the Hipparcos consortium who discussed the calculation, transformation matrix and error propagation. We would like to give only a short description of the error estimation. The general equation for the variance of a function of several variables is used for this purpose. That formula is true only if the covariances are zero (the errors are uncorrelated). That assumption is fulfilled since the two proper-motion components are measured independently. Furthermore it is assumed that only the radial velocity, proper motions and parallax contribute to the error distribution. For nearby stars (about 25 pc) an error of the proper motions of about $\pm 3\,\mathrm{mas\,yr^{-1}}$ (most of the Hipparcos measurements are a factor three better than that) corresponds to an uncertainty in the transverse motion of only about $0.5\,\mathrm{km\,s^{-1}}$; it is clear that the errors of the radial velocities are much more significant.

The radial velocities for our program stars are listed in Table 6. The following references were used for that Table: Wilson (1953), Evans (1967), Batten, Fletcher & MacCarthy (1989), Barbier-Brossat, Petit & Figon (1994), Duflot et al. (1995), Hauck et al. (1995, 1998), Fehrenbach et al. (1996, 1997), Nordström et al. (1997) and Grenier et al. (1999a,b). The mean and the error of the mean were calculated without weighting the individual measurements. From Table 6 only three stars (HD 319, HD 110411 and HD 204041) show evidence for variable radial velocities but no prominent photometric or spectroscopic variability has been detected so far. Moreover, Table 6 lists the kinematic data for the program λ Boötis stars from the Hipparcos database. The investigated sample is limited in distance (≈ 220 pc) because of the lack of Hipparcos data and/or radial velocities for more distant objects. No star exceeds $|V| = 50\,\mathrm{km\,s^{-1}}$ and the sample is very homogeneously distributed. A similar conclusion is given by Gómez et al. (1998a) for classical CP

stars as well as by Gómez et al. (1998b) for a small sample of λ Boötis stars.

We have compared the velocities of stars in our λ Boötis sample with the results of Caloi et al. (1999). They studied the relationship between the kinematics, age and heavy-element content for the solar neighbourhood, using the Hipparcos data. For $V < -40\,\mathrm{km\,s^{-1}}$, $|U| > +60\,\mathrm{km\,s^{-1}}$ and $|W| > +30\,\mathrm{km\,s^{-1}}$, the minimum stellar age is about 2 Gyr. Only two of the λ Boötis stars would meet the V criterion, HD 6870 ($V = -41.7(2.8)\,\mathrm{km\,s^{-1}}$) and HD 84123 ($V = -45.4(4.4)\,\mathrm{km\,s^{-1}}$), but their U and W velocities (like those of all other stars in the sample) are well below the limits given. Overall, the velocities are typical of true Population I objects.

The comparison with the sample of normal stars (Fig. 9) shows very good agreement between the two distributions. They agree at significance levels of 72% (U), 74% (V) and 97% (W).

Notice that Faraggiana & Bonifacio (1999) made a similar analysis for a different sample of candidate λ Boötis stars (see Section 4 therein). They only investigated the parameter $(U^2+W^2)^{1/2}$ which is a measure of the kinematic energy not associated with Galactic rotation. They come to the conclusion that all of their program stars are qualified as disk members. Since they give no individual values for the space motions and radial velocities, we are not able to compare our results with theirs.

7 CONCLUSIONS

We have used all currently available photometric data as well as Hipparcos data to determine astrophysical parameters such as the effective temperatures, surface gravities and luminosities. As a next step, masses and ages were calibrated within appropriate post-MS evolutionary models. Furthermore, Galactic space motions were calculated with the help of radial velocities from the literature. The comparison with already published results shows good agreement of the derived parameters. All results were compared with those of a test sample of normal-type objects in the same spectral range chosen in order to match the $(B-V)_0$ distribution of the λ Boötis group. From a comprehensive statistical analysis we conclude:

- The standard photometric calibrations within the Johnson *UBV*, Strömgren *uvbyβ* and Geneva 7-colour systems are valid for this group of chemically peculiar stars.
- The group of λ Boötis stars consists of true Population I objects which can be found over the whole area of the MS with a peak at a rather evolved stage (≈ 1 Gyr). That is in line with the distribution of the test sample.
- The λ Boötis type group is not significantly distinct from normal stars except, possibly, by having slightly lower temperatures and masses for $t_{\rm rel} > 0.8$. The $v \sin i$ range is rather narrow throughout the MS with a mean value of about $120\,\mathrm{kms^{-1}}$.
- There seems to exist a non-uniform distribution of effective temperatures for group members with a large proportion of objects (more than 70%) cooler than 8000 K.
- It seems that objects with peculiar hydrogen-line profiles are preferentially found among later stages of stellar evolution.
- No correlation of age with elemental abundance or projected rotational velocity has been detected.
- A comparison of the stellar Na abundances with nearby IS sight lines hints at an interaction between the λ Boötis stars and the ISM.
- There is one single mechanism responsible for the observed phenomenon which produces moderate to strong underabundances working continuously from very early (10 Myr) to very late evolutionary stages (2.5 Gyr). It produces the same absolute abundances throughout the MS lifetime for 2% of all luminosity class V objects with effective temperatures from 10500 K to 6500 K.
- The current list of stars seem to define a very homogeneous group, validating the proposed membership criteria in the optical and UV region.

These rather strict observational results for a significant number of λ Boötis stars will need to be taken into account in future work on theories and models trying to explain the phenomenon. The constraints presented here will help considerably to reduce the number of free parameters in the models and finally to provide a critical test for them.

Acknowledgements. This work was partly supported by the Fonds zur Förderung der wissenschaftlichen Forschung, project P14984 and it is dedicated to G. Derka who died during its preparation. Use was made of the SIMBAD database, operated at CDS, Strasbourg, France and the GCPD database, operated at the Institute of Astronomy of the University of Lausanne.

REFERENCES

Abt H.A., Morrell N.I., 1995, ApJS, 99, 135
Adelman S.J., 1991, MNRAS, 252, 116
Adelman S.J., 1994, MNRAS, 271, 355
Adelman S.J., 1996, MNRAS, 280, 130
Adelman S.J., Bolcal C., Hill G., Kocer D., 1991, MNRAS, 252, 329
Adelman S.J., Caliskan H., Kocer D., Bolcal C., 1997, MNRAS, 288, 470
Andrievsky S.M., Chernyshova I.V., Ivashchenko O.V., 1995, A&A, 297, 356
Andrievsky S.M., Chernyshova I.V., Korotin S.A., et al., 2002, A&A (in preparation)
Andrillat Y., Jaschek C., Jaschek M., 1995, A&A, 299, 493
Arenou F., Grenon M., Gómez A., 1992, A&A 258, 104
Barbier-Brossat M., Petit M., Figon P., 1994, A&AS, 108, 603
Batten A.H., Fletcher J.M., MacCarthy D.G., 1989, Publ. Dominion Astrophys. Obs., 17
Bohlender D.A., Gonzalez J.F., Matthews J.M., 1999, A&A, 350, 553
Caliskan H., Adelman S.J., 1997, MNRAS, 288, 501
Caloi V., Cardini D., D'Antona F., Badiali M., Emanuele A., Mazzitelli I., 1999, A&A, 351, 925
Cayrel de Strobel G., 1996, A&AR, 7, 243
Chen B., Vergely J.L., Valette B., Carraro G., 1998, A&A, 336, 137
Chernyshova I.V., Andrievsky S.M., Kovtyukh V.V., Mkrtichian D.E., 1998, Contributions of the Astronomical Observatory Skalnaté Pleso, Vol. 27, No. 3, p. 332
Claret A., 1995, A&AS, 109, 441
Cowley C.R., 1995, PASPC, 81, 467
Cowley C.R., Sears R.L., Aikman G.C.L., Sadakane K., 1982, ApJ, 254, 191

Drilling J.S., Landolt A.U., 2000, in A.N. Cox, ed, Allen's Astrophysical Quantities, 4th edition, Springer Verlag, p. 388
Duflot M., Fehrenbach Ch., Mannone C., Burnage R., Genty V., 1995, A&AS, 120, 177
Evans D.S., 1967, Catalogue of stellar radial velocities, IAU Symp. 30, 5
Faraggiana R., Bonifacio P., 1999, A&A, 349, 521
Faraggiana R., Gerbaldi M., 1998, Contributions of the Astronomical Observatory Skalnaté Pleso, Vol. 27, No. 3, p. 413
Fehrenbach Ch., Duflot M., Genty V., Amieux G., 1996, Bull. Inform. CDS 48, 11
Fehrenbach Ch., Duflot M., Mannone C., Burnage R., Genty V., 1997, A&AS, 124, 255
Garrison R.F., Gray R.O., 1994, AJ, 107, 1556
Gómez A.E., Luri X, Grenier S., et al., 1998a, A&A, 336, 953
Gómez A.E., Luri X, Sabas V., et al., 1998b, Contributions of the Astronomical Observatory Skalnaté Pleso, Vol. 27, No. 3, p. 171
Gray R.O., 1988, AJ, 95, 220
Gray R.O., 1989, AJ, 98, 1049
Gray R.O., Corbally C.J., 1993, AJ, 106, 632
Gray R.O., Corbally C.J., 1998, AJ, 116, 2530
Gray R.O., Corbally C.J., 1999, AAS, 195, 4702
Gray R.O., Garrison R.F., 1987, ApJS, 65, 581
Gray R.O., Garrison R.F., 1989a, ApJS, 69, 301
Gray R.O., Garrison R.F., 1989b, ApJS, 70, 623
Grenier S., Burnage R., Faraggiana R., et al., 1999a, A&AS, 135, 503
Grenier S., Baylac M.O., Rolland L., et al., 1999b, A&AS, 137, 451
Hakkila J., Myers J.M., Stidham B.J., Hartmann D.H., 1997, AJ, 114, 2043
Hauck B., Ballereau D., Chauville J., 1995, A&AS, 109, 505
Hauck B., Ballereau D., Chauville J., 1998, A&AS, 128, 429
Heiter U., 2000, PASP, 112, 1509
Heiter U., 2002, A&A, 381, 959
Heiter U., Kupka F., Paunzen E., Weiss W.W., Gelbmann M., 1998, A&A, 335, 1009
Heiter U., Weiss W.W., Paunzen E., 2002, A&A, 381, 971
Hill G.M., 1995, A&A, 294, 536
Hill G.M., Landstreet J.D., 1993, A&A, 276, 142
Holweger H., Rentzsch-Holm I., 1995, A&A, 303, 819
Holweger H., Hempel M., Kamp I., 1999, A&A, 350, 603
Iliev I.K., Barzova I.S., 1993, Ap&SS, 208, 277
Iliev I.K., Barzova I.S., 1995, A&A, 302, 735
Iliev I.K., Paunzen E., Barzova I.S., et al., 2002, A&A, 381, 914
Jaschek M., Andrillat Y., Jaschek C, 1989, A&A, 218, 180
Johnson D.R.H., Soderblom D.R., 1987, AJ, 93, 864
Kamp I., Iliev I.Kh., Paunzen E., et al., 2001, A&A, 375, 899
King J.R., 1994, MNRAS, 269, 209
Kobi D., North P., 1990, A&AS, 85, 999
Koen C., 1992, MNRAS, 256, 65
Künzli M., North P., Kurucz R.L., Nicolet B., 1997, A&AS, 122, 51
Mihalas D., Routly P.M., 1968, Galactic Astronomy, Freeman & Co., San Francisco, p. 101
Moon T.T., Dworetsky M.M., 1985, MNRAS, 217, 305
Morel P., 1997, A&AS, 124, 597
Napiwotzki R., Schönberner D., Wenske V., 1993, A&A, 268, 653
Nordström B., Stefanik R.P., Latham D.W., Andersen J., 1997, A&AS, 126, 21
Oudmaijer R.D., Groenewegen M.A.T., Schrijver H., 1998, MNRAS, 294, L41
Palla F., Stahler S.W., 1993, ApJ, 418, 414
Paunzen E., 1997, A&A, 326, L29
Paunzen E., 2001, A&A, 373, 633
Paunzen E., Gray R.O., 1997, A&AS, 126, 407
Paunzen E., Kamp I., Iliev I.Kh., et al., 1999a, A&A, 351, 981
Paunzen E., Andrievsky S.M., Chernyshova I.V., Klochkova V.G., Panchuk V.E., Handler G., 1999b, A&A, 351, 981
Perryman M.A.C., Høg E., Kovalevsky J., Lindegren L., Turon C., 1997, The Hipparcos and Tycho Catalogues, ESA SP-1200
Preston G.W., 1974, ARA&A, 12, 257
Rees D.G., 1987, Foundations of Statistics, Chapman & Hall, London
Sandage A., 1972, ApJ, 178, 1
Schaller G., Schaerer D., Meynet G., Maeder A., 1992, A&AS, 96, 269
Sfeir D.M., Lallement R., Crifo F., Welsh B.Y., 1999, A&A, 346, 785
Slettebak A., Kuzma T.J., Collins G.W., 1980, ApJ, 242, 171
Solano E., Paunzen E., 1999, A&A, 348, 825
Solano E., Paunzen E., Pintado O.I., Varela J., 2001, A&A, 374, 957
Stürenburg S., 1993, A&A, 277, 139
Turcotte S., Charbonneau P., 1993, ApJ, 486, 536
Uesugi A., Fukuda I., 1982, Revised Catalogue of Stellar Rotational Velocities, Department of Astronomy, Kyoto Univ., Kyoto
van Winckel H., Waelkens C., Waters L.B.F.M., 1995, A&A, 297, 25
Varenne O., Monier R., 1999, A&A, 351, 247
Venn K.A., Lambert D.L., 1990, ApJ, 363, 234
Vergely J.-L., Freire Ferrero R., Siebert A., Valette B., 2001, A&A, 366, 1016
Welsh B.Y., Crifo F., Lallement R., 1998, A&A, 333, 101
Wilson R.F., 1953, General Catalogue of stellar radial velocity, Carnegie Inst. of Washington, Publ. 601
Wolff S.C., 1983, The A-type Stars: Problems and Prospectives, NASA-SP 463